Iranian Journal of Chemical Engineering

Journal Homepage: www.ijche.com

pISSN: 1735-5397
eISSN: 2008-2355

# Investigating Parameters Effective on Purity Purification of Graphite Recycled from Spent Lithium-Ion Batteries

**Ramin Badrnezhad, Mohammad Mahdi Bahri, Mobin Gharemanlo, Mehrdad Shourehkandi, Shahram Ghanbari Pakdehi*, Maryam Farid Mohammadi**

*Department of Chemical Engineering, Faculty of Chemistry and Chemical Engineering, Malek Ashtar University of Technology, Tehran, Iran*

**ARTICLE INFO**

**Article type:**
Research article

**Article history:**
*Received: 2026-01-25*
*Revised: 2026-02-10*
*Accepted: 2026-02-25*
*Available online: 2026-02-26*

**Keywords:**
*Lithium-ion battery,*
*Graphite recovery,*
*Primary/secondary leaching,*
*Electrochemical behavior*

**ABSTRACT**

*Lithium-ion batteries are widely used in various electronic devices and typically discarded after their service life, causing significant environmental damage and resource wastage. Therefore, recycling the valuable components of the batteries, such as graphite, is essential. Graphite, employed as the anode material, is one of the key components targeted for recovery. In graphite recycling operations from spent batteries, critical hydrometallurgical processes are primary and secondary leaching stages using sulfuric acid. In this research, both leaching processes were systematically optimized. The optimal conditions identified for primary leaching were the temperature of 77 °C, concentration of 1.75 M of sulfuric acid, leaching duration of 4 hours, and liquid-to-solid graphite powder ratio of 5. Under these conditions, the graphite purity after the primary leaching process was 99.56 wt%. Subsequently, in the secondary leaching stage, a final high purity of 99.98% was achieved for the graphite product. To evaluate the electrochemical performance of the recycled graphite, galvanostatic charge-discharge tests, which demonstrated the specific capacity of 350 mAh/g, were conducted. This capacity is comparable to that of the commercial graphite, confirming the effectiveness of the developed recycling process.*

DOI: 10.22034/ijche.2026.553020.1577 URL: https://www.ijche.com/article_243088.html

## 1. Introduction

Today, lithium-ion batteries are widely used in portable electronic products, electric vehicles, entertainment equipment, medical industries, and many more due to their high operating voltage, high energy density, and excellent cycle performance. Lithium-ion batteries contain plastics, organic compounds, heavy

*Corresponding author: sh_ghanbari73@yahoo.com

metals, etc. Some of these materials are flammable, while others are toxic. Therefore, recycling lithium-ion batteries is crucial for environmental protection and also contributes to the sustainable use of resources [1,2]. Research on the recovery of spent lithium-ion batteries primarily focuses on the cathode, as the precious metals in the cathode offer high economic and environmental benefits. Graphite (as the anode) is considered one of the most important materials in lithium-ion batteries due to its extensive use. On the other hand, the amount of graphite in spent lithium-ion batteries varies from 12 wt% to 21 wt%. Therefore, with the increase in the quantity of spent lithium-ion batteries, the amount of graphite will significantly rise [3,4]. Lithium-ion batteries mainly consist of 25-30 wt% cathode materials, 15-17 wt% anode materials, 10-15 wt% electrolyte, and 4-10 wt% organic separators [5,6]. Anode materials account for 5-15% of the total cost of lithium-ion batteries, and graphite is the primary anode material due to its long-term cycle stability, high electrical conductivity, thermal and mechanical stability, and honeycomb structure. The price of battery-grade graphite was estimated at $5,000 to $20,000 per ton in 2016. This evidence suggests that the spent graphite could be an important source of low-cost graphite in the near future. Consequently, from economic and environmental perspectives, the spent graphite should be recycled. Recovering graphite from spent lithium-ion batteries can eliminate environmental pollution and bring certain economic benefits [7].

The surface and interlayer of the spent graphite are often contaminated with various organic and inorganic compounds during regular battery use. These impurities are typically present in the electrolyte solution, especially in organic solvents, and can contaminate the electrode materials, thereby limiting their recovery and reuse [8]. Recycling the spent graphite from spent lithium-ion batteries usually involves three stages [8]:

a) Separation of black powder from anode parts or cathode/anode scraps of spent batteries

b) Purification and structural modification of the spent graphite

c) Reuse for lithium-ion battery anodes or production of new materials

After collecting, sorting, and separating spent lithium-ion batteries, various physical processes are performed on them. These processes include crushing, milling, sieving, and physical separation. This stage (known as pretreatment) is a prerequisite for leaching and purification steps. Pretreatment generally includes electrical discharge and battery disassembly. The electrical discharge process ensures safety in the subsequent recovery process, as there are hazards [9,10]. In general, the product of the pretreatment stage is anode pieces or a mixture of anode and cathode, depending on the type of pretreatment process [8]. After separating graphite from other components of spent lithium-ion batteries, the obtained graphite usually cannot meet battery industry standards due to impurities and structural defects. Currently, hydrometallurgical, pyrometallurgical, and combined processes are mainly used for purifying the spent graphite and regenerating it for batteries [11]. Recovery through leaching operations is one of the most common methods in the industry of recycling for spent lithium-ion batteries due to its selectivity. Nitric acid, sulfuric acid, hydrochloric acid, and other strong acids have been used as leaching agents for electrode materials, with hydrogen peroxide as a reducing agent. Most cathode materials and metallic impurities are dissolved during leaching operations, while graphite remains solid and can be recovered using filtration. The graphite can then undergo a secondary leaching process to remove remaining metals from its structure, yielding

high-purity graphite that can subsequently be used for various applications [12]. To date, water, acids (HCl, $H_2SO_4$, and citric acid), and ammonium per-sulfate have been used for recovering graphite. Leaching with water can remove many impurities, including water-soluble lithium and solid electrolyte phase in the spent graphite. Based on the obtained results, traces of lithium salts and iron ions remain in the recycled graphite after water leaching. In fact, the primary forms of lithium in the spent graphite are $Li_2CO_3$, $Li_2O$, LiF, $LiPF_6$, $ROCO_2Li$, and $CH_3OLi$. Some water-soluble lithium compounds like $CH_3OLi$ and $Li_2O$ can be removed with water. However, other water-insoluble lithium compounds like LiF and $ROCO_2Li$ are difficult to be removed with simple water leaching [11]. Pyrometallurgy is another common process for removing impurities and recovering the crystalline network of the spent graphite. This operation oxidizes and separates metallic impurities accompanying graphite at high temperatures and also regenerates the overall graphite structure for reuse in lithium-ion batteries. The advantage of this method is that no chemical solutions are added to the process, saving costs in pollution removal operations. However, these processes have long operation times and high energy consumption. Additionally, the recycled graphite will have low purity and limited usability. For this reason, in most sources, this operation is combined with leaching processes, turning the spent graphite into graphite suitable for reuse in lithium-ion batteries [11,12]. In general, leaching operations are mainly used to remove metals and organic impurities in the spent graphite, while pyrometallurgy is efficient for regenerating its structure. Therefore, combining leaching and pyrometallurgy is considered a more efficient approach for regenerating the spent graphite. The combined method of leaching with heat treatment is good for graphite recovery, and the high-temperature heat treatment of the spent graphite shows better performance than low-temperature operations, which can be attributed to improved crystallinity [11,12]. Yang et al. [4] and Yang Guo et al. [13] separated graphite and lithium, using heat treatment at 400 °C and leaching with hydrochloric acid. Zhang et al. [14] and Zhao et al. [15] used a modified process combining fluorination roasting and leaching with sulfuric acid to recover graphite from lithium-ion batteries. Liu et al. [16] and Ma et al. [17] also recycled graphite for reuse in lithium-ion batteries, using alkaline roasting and leaching. Gao et al. [18] and Yang et al. [19] investigated the regeneration of the spent graphite from spent lithium-ion batteries by leaching and high-temperature heat treatment for reuse in lithium-ion batteries. Other methods reported in literature include electrochemical methods [20], carbon coating [21,22], and flotation [23], which are not suitable for recycling industrial batteries.

In published research, recycled graphite has fewer impurities. In this study, a simple method for recycling graphite with high impurities from lithium-ion battery recycling unit will be presented. The effects of various parameters on the purity of the recycled graphite and their optimization in the used process will be examined.

## 2. Materials and methods

### 2.1. Materials

The chemicals used include: sulfuric acid solution (95-97% pure), nitric acid (65% pure), acetic acid (96% pure), and deionized water. All used acids have been obtained from Merck, Germany. The graphite used in this research was supplied by the Iranian Energy Resources Development Organization in powder form. As it is seen in Figure 1, the black powder

includes separators, organic binders, and residual electrolyte.

**Figure 1.** Graphite feed received from the Iranian Energy Resources Development Organization.

### 2.2. Equipment used

The major equipment used in this research includes: a heater-stirrer (Heidolph, model MR300K), a dryer or oven for reducing sample moisture (UMB400, Memmert), a 30-mesh sieve (ASTM E11, Damavand), a furnace for sample calcination (Andreh), a high-precision digital balance (±0.001 g) (Mettler model PB6-S), and an electrochemical testing system (Zive model SP1).

### 2.3. Experimental procedure

Since the spent graphite contains a large amount of plastic (plastics related to battery separators), it should first undergo pretreatment. In the pretreatment stage, the spent graphite is placed in a dryer at 120 °C for 2 hours to evaporate the moisture. Then, the dried graphite is placed in a mill for two hours to crush any clumps and enable sieving in the next stage. The resulting powder is passed through a 30-mesh sieve to separate the plastics. The graphite that passes through the sieve is placed in a furnace at 450 °C for 4 hours to decompose and evaporate any remaining plastics. The powder obtained from this stage undergoes leaching with sulfuric acid under the certain conditions. In the leaching stage, four parameters, including the solid-to-liquid ratio(S/L), number of washing time, concentration of the acid and leaching temperature, were optimized based on the minimum and maximum values mentioned in the sources. The leaching is carried out in a vessel with a mechanical mixer of 200 rpm. After leaching, the graphite-containing solution undergoes filtration. The resulting solid graphite is washed with distilled water. Subsequently, the obtained graphite is impregnated with a small amount of sulfuric acid and undergoes sulfation roasting in a furnace. The roasted graphite undergoes leaching again, and this cycle is repeated three times. The product from the final leaching stage is filtered and enters the dryer. The obtained graphite is evaluated for purity, structure, and electrochemical properties for use in lithium-ion battery anodes. An overview of recycling graphite is shown in Figure 2.

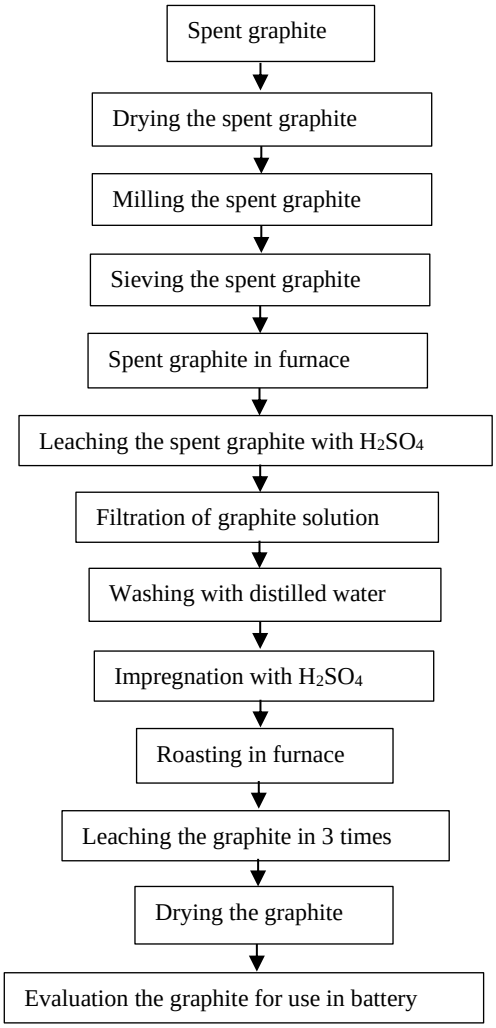


**Figure 2.** Overview of the graphite recycling process from spent lithium-ion batteries

### 2.4. Analysis

The analytical devices used in this research include: X-ray diffractometer (XRD) (Rigaku D/Max-RBL) to determine the crystalline structure, crystallinity degree, crystal diameter of particles, and phase types in graphite. Inductively coupled plasma (ICP) spectroscope (Perkin Elmer Optima 5300 DV) to identify elements in the sample and measure their concentrations.

In the overall process for recovering graphite, lithium-ion batteries available in the market are first collected and undergo crushing operations. Battery casing plastics are separated. Then, metallic components are extracted in leaching operations. The resulting graphite (as feed) has the composition according to Table 1. As it is seen, the graphite feed contains about 11.5% impurities that should be separated.

**Table 1.**
Percentage of impurities in the spent graphite feed.

| Ingredients in feed | Li | Al | Mn | Cu | Ni | Co | C |
|---|---|---|---|---|---|---|---|
| wt% | 0.305 | 0.270 | 1.258 | 1.800 | 1.530 | 6.320 | 88.510 |

## 3. Results and discussion

As mentioned in the introduction of this research, leaching with various acids is a suitable way to separate metallic impurities from the graphite feed. Based on studies and literature, various acids were used to reduce impurities in graphite. In this research, in initial experiments, leaching of the impurities from graphite was performed with the 1.75 M sulfuric acid solution under the conditions of the temperature of 77 °C, duration of 4 hours, and solid graphite mass to sulfuric acid solution ratio (S/L) of 10. The resulting graphite is called ASG. Leaching with the 1 M nitric acid solution was performed under the conditions of the temperature of 80 °C, duration of 75 minutes, and solid graphite mass to nitric acid solution ratio (S/L) of 28. The resulting graphite is called ANG. Leaching with the 1.5 M hydrochloric acid solution was performed under the conditions of the temperature of 80 °C, duration of 4 hours, and solid graphite mass to hydrochloric acid solution ratio (S/L) of 20. The resulting graphite is called AHG. The ICP results of leaching with the three mentioned acids are presented in Table 2. Additionally, the analyses of the spent graphite samples (called SG) and commercial graphite samples (shown as CG) are provided for comparison.

By comparing Tables 1 and 2, it is observed that among the three acids used for leaching (nitric acid, sulfuric acid, and hydrochloric acid), nitric acid has higher efficiency in removing impurities but requires more resistant equipment due to high corrosiveness, resulting in higher costs. The wastewater from nitric acid leaching contains metal nitrates, requiring more complex treatment methods to reduce environmental risks. Sulfuric acid is recommended for industrial applications due to better availability, lower price, and less corrosion of equipment. This acid brings lower costs and higher safety on larger production scales, and its wastewater, containing metal sulfates, can be controlled with appropriate treatments [13].

**Table 2.**
ICP results of impurities in the graphite obtained from leaching with three acids: sulfuric, nitric, and hydrochloric acids.

| Components / Amount of components in graphite type (ppm) | Li | Al | Mn | Cu | Ni | Co | C |
|---|---|---|---|---|---|---|---|
| Spent graphite (SG) | 3050 | 2700 | 12580 | 18000 | 15300 | 63200 | 885100 |
| Leaching with sulfuric acid agent (ASG) | 5 | 85 | 205 | 509 | 1784 | 1.529 | 995800 |
| Leaching with nitric acid agent (ANG) | 77 | 106 | 112 | 462 | 1129 | 942 | 997100 |
| Leaching with hydrochloric acid agent (AHG) | 582.6 | 264.8 | 176.6 | 529.7 | 2824.9 | 3001.4 | 992600 |
| Commercial graphite (CG) | 1.9> | 9.500 | 1.9> | 9.5 | 1.9> | 19 | 999900< |

As it is seen in Table 2, lithium and aluminum are almost completely removed. Since these two elements are easily removed from the spent graphite, the focus in subsequent stages is on removing cobalt, manganese, nickel, and copper. To remove the mentioned impurities, leaching with sulfuric acid is necessary. For this purpose, a series of experiments was carried out to reduce the mentioned impurities. To speed up and reduce experimental costs, an experimental design was used.

For optimizing the leaching process parameters, the response surface methodology (RSM) was employed. In this method, independent variables, including the temperature, concentration of the acid, time, and acid-to-solid graphite powder ratio (L/S), were considered as main factors. To examine the simultaneous effects of multiple factors and their interactions, the central composite design (CCD) was used. In this case, it can be determined which variables have the greatest impact on the system response [24,25]. The Design Expert 10.0.0 software was used for the experimental design. Accordingly, the main factors and their different levels were entered into the software.

The parameter ranges are presented in Table 3. Table 4 shows the number of the designed experiments for separating impurities from the feed graphite (coded as ASG). As it is observed, the number of experiments is 26. Based on Table 4, tests were performed, and the results are presented in Table 5.

**Table 3.**
Parameter ranges in the experimental design for removing impurities.

| Parameter | Sign | Upper limit | Lower limit |
|---|---|---|---|
| T(°C) | A | 95 | 25 |
| Concentration of sulfuric acid solution (M) | B | 4 | 1 |
| Washing time (hr) | C | 5 | 1 |
| Ratio of the sulfuric acid solution to the mass of graphite(L/S) | D | 8 | 4 |

**Table 4.**
Experimental designs to determine optimal conditions.

| Sample No. | L/S (D) | Washing time (C) | Acid concentration (B) | Temperature (A) |
|---|---|---|---|---|
| 1 | 5 | 2 | 1.75 | 42.5 |
| 2 | 5 | 2 | 1.75 | 77.5 |
| 3 | 5 | 2 | 3.25 | 42.5 |
| 4 | 5 | 2 | 3.25 | 77.5 |
| 5 | 5 | 4 | 1.75 | 42.5 |
| 6 | 5 | 4 | 1.75 | 77.5 |
| 7 | 5 | 4 | 3.25 | 42.5 |
| 8 | 5 | 4 | 3.25 | 77.5 |
| 9 | 7 | 2 | 1.75 | 42.5 |
| 10 | 7 | 2 | 1.75 | 77.5 |
| 11 | 7 | 2 | 3.25 | 42.5 |
| 12 | 7 | 2 | 3.25 | 77.5 |
| 13 | 7 | 4 | 1.75 | 42.5 |
| 14 | 7 | 4 | 1.75 | 77.5 |
| 15 | 7 | 4 | 3.25 | 42.5 |
| 16 | 7 | 4 | 3.25 | 77.5 |
| 17 | 6 | 3 | 2.5 | 25 |
| 18 | 6 | 3 | 2.5 | 95 |
| 19 | 6 | 3 | 1 | 60 |
| 20 | 6 | 3 | 4 | 60 |
| 21 | 6 | 1 | 2.5 | 60 |
| 22 | 6 | 5 | 2.5 | 60 |
| 23 | 4 | 3 | 2.5 | 60 |
| 24 | 8 | 3 | 2.5 | 60 |
| 25 | 6 | 3 | 2.5 | 60 |
| 26 | 6 | 3 | 2.5 | 60 |

**Table 5.**
Test results based on Table 4 and the graphite purity and amount of impurity components.

| Sample No. | Cu (ppm) | Ni (ppm) | Co (ppm) | Mn (ppm) | Graphite purity (wt%) |
|---|---|---|---|---|---|
| 1 | 2832.1 | 3068.1 | 41064.9 | 4625.7 | 99.07 |
| 2 | 724.6 | 2173.7 | 3260.6 | 217.4 | 99.52 |
| 3 | 1482.2 | 2964.4 | 5928.9 | 296.4 | 99.31 |
| 4 | 594.8 | 2329.7 | 2478.4 | 39.7 | 99.20 |
| 5 | 513.9 | 1631.3 | 2039.2 | 0 | 99.20 |
| 6 | 550.2 | 2063.1 | 2701.6 | 39.3 | 99.55 |
| 7 | 1107.2 | 2860.3 | 4613.4 | 332.2 | 99.46 |
| 8 | 671.5 | 2878 | 2906.8 | 48 | 99.46 |
| 9 | 511.6 | 1672.4 | 2065.9 | 295 | 99.10 |
| 10 | 1312.8 | 3657.2 | 5814 | 290.7 | 98.86 |
| 11 | 1733.4 | 3370.6 | 4237.3 | 128.9 | 98.75 |
| 12 | 622.7 | 1027.4 | 1556.7 | 0 | 99.36 |
| 13 | 625.8 | 2792.2 | 5343.7 | 192.6 | 99.00 |
| 14 | 460.2 | 1932.8 | 1435.8 | 55.2 | 99.38 |
| 15 | 1261.8 | 4076.5 | 2426.5 | 194.1 | 98.92 |
| 16 | 509.9 | 1784.7 | 1529.7 | 25.5 | 98.97 |
| 17 | 1216.9 | 3017.9 | 4867.6 | 292.1 | 99.00 |
| 18 | 2149.6 | 3095.4 | 3267.4 | 0 | 98.93 |
| 19 | 758.6 | 2749.9 | 3508.4 | 24.7 | 99.02 |
| 20 | 546.9 | 2050.9 | 2643.3 | 45.6 | 99.55 |
| 21 | 640 | 2000 | 2240 | 0 | 99.26 |
| 22 | 622.7 | 1027.4 | 1556.7 | 0 | 99.26 |
| 23 | 52.3 | 83.6 | 167.2 | 0 | 99.06 |
| 24 | 949.4 | 2943.1 | 2563.7 | 0 | 99.39 |
| 25 | 859.6 | 1661.9 | 3438.4 | 0 | 99.24 |
| 26 | 1322.8 | 1940 | 2733.7 | 0 | 99.24 |

According to the analysis of variance in Table 6, the modified cubic model has the lowest P value and the highest correlation coefficient. According to the Table, all terms also have acceptable P values of below 1.0. However, to maintain the hierarchy of the model, terms A and $B^2$, which have P values of above 1.0, were retained.

**Table 6.**
Modified 3rd order ANOVA table.

| Source | Sum of squares | Degree of freedom | Mean squares | F-value | p-value |
|---|---|---|---|---|---|
| Model | 1.17 | 18 | 0.0653 | 23.19 | 0.0123 |
| A | 0.0024 | 1 | 0.0024 | 0.8706 | 0.4196 |
| B | 0.1405 | 1 | 0.1405 | 49.91 | 0.0058 |
| C | 0.0109 | 1 | 0.0109 | 3.88 | 0.1435 |
| D | 0.2282 | 1 | 0.2282 | 81.08 | 0.0029 |
| AB | 0.0415 | 1 | 0.0415 | 14.76 | 0.0311 |
| AC | 0.0840 | 1 | 0.0840 | 29.84 | 0.0121 |
| AD | 0.0884 | 1 | 0.0884 | 31.40 | 0.0112 |
| BC | 0.0415 | 1 | 0.0415 | 14.76 | 0.0311 |
| BD | 0.0385 | 1 | 0.0385 | 13.70 | 0.0343 |
| CD | 0.0431 | 1 | 0.0431 | 15.31 | 0.0297 |
| $A^2$ | 0.1084 | 1 | 0.1084 | 38.53 | 0.0084 |
| $B^2$ | 0.0002 | 1 | 0.0002 | 0.0722 | 0.8056 |
| $D^2$ | 0.1036 | 1 | 0.1036 | 36.83 | 0.0090 |
| ABC | 0.0409 | 1 | 0.0409 | 14.54 | 0.0317 |
| ABD | 0.0568 | 1 | 0.0568 | 20.18 | 0.0206 |
| BCD | 0.0352 | 1 | 0.0352 | 12.51 | 0.0385 |
| $A^2B$ | 0.1015 | 1 | 0.1015 | 36.07 | 0.0092 |
| $AB^2$ | 0.0435 | 1 | 0.0435 | 15.46 | 0.0293 |
| Residual | 0.0084 | 3 | 0.0028 | | |
| Fit defect | 0.0084 | 2 | 0.0042 | | |
| Net error | 0.0000 | 1 | 0.0000 | | |
| Summation | 1.18 | 21 | | | |

Residual plots are given in Figure 3. According to Figure 3 (a), which demonstrates the normal probability plot in terms of the internal Studentized residuals, in the normal case the residuals should follow a straight line; otherwise, the responses should be these plots, the responses should be transformed. transformed. In Figure 3 (b), the Studentized residuals are also plotted in terms of the predicted responses. In the normal case, the residuals have constant variance; otherwise, if the scatterplot resembles a "<" shape, it needs to be transformed. In general, according to

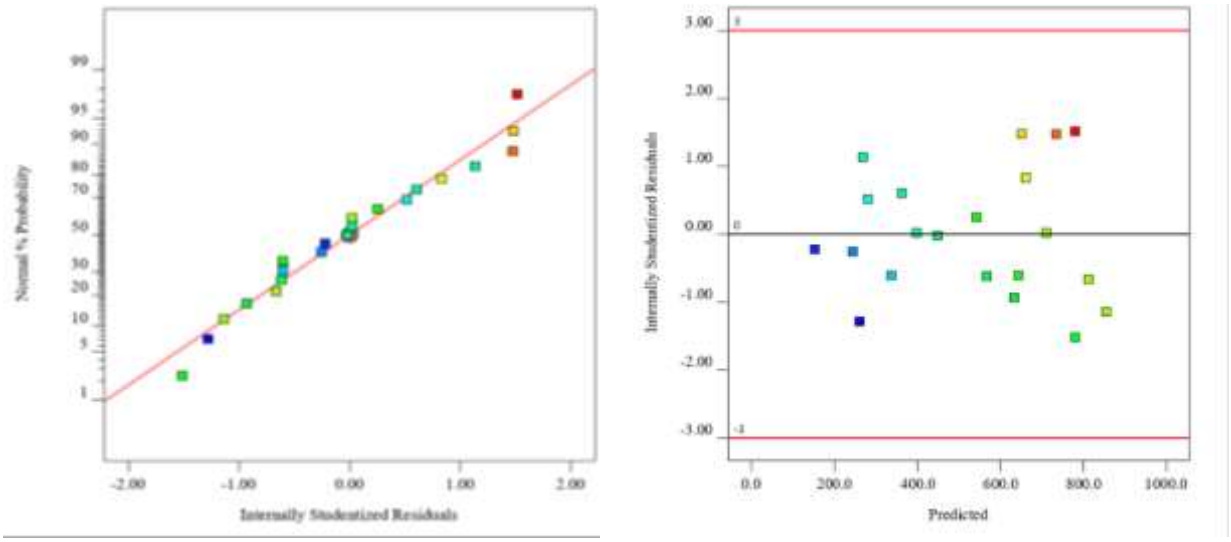


**(a)** **(b)**

**Figure 3.** (a) Normal residual plot, and (b) residual plot in terms of the predicted response.

After performing transformations and the analysis of variance (ANOVA), parameters with high p-values were removed from the model to make the model meaningful. In addition, according to the graph of actual and predicted responses, the presence of outliers was observed; therefore, these data were also manually removed from the analysis process.

Considering the plot of residuals and actual values in Figure 4, the constant variance observed in the data suggests that no transformation is required. The results of the analysis of variance (ANOVA) show that the temperature and concentration of sulfuric acid have a significant effect on the leaching efficiency, while the reaction time and solid to liquid ratio have less impact.

The response surface diagrams, related to the effect of parameters on copper, nickel, cobalt, and manganese, are shown in Figure 5.

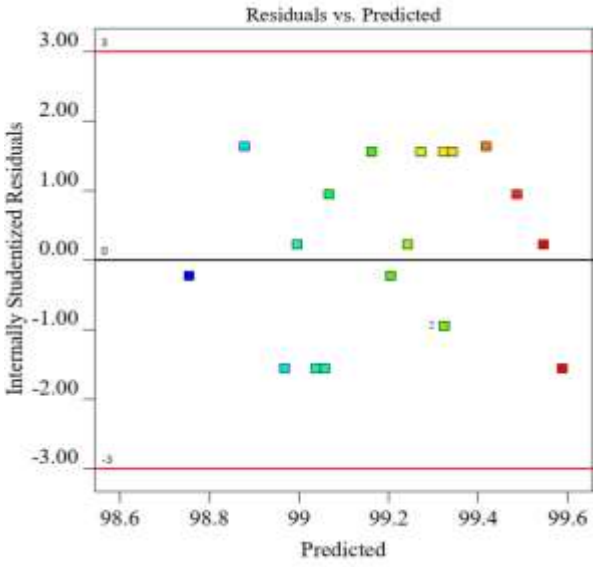


**Figure 4.** Plot of Studentized residuals versus predicted responses.

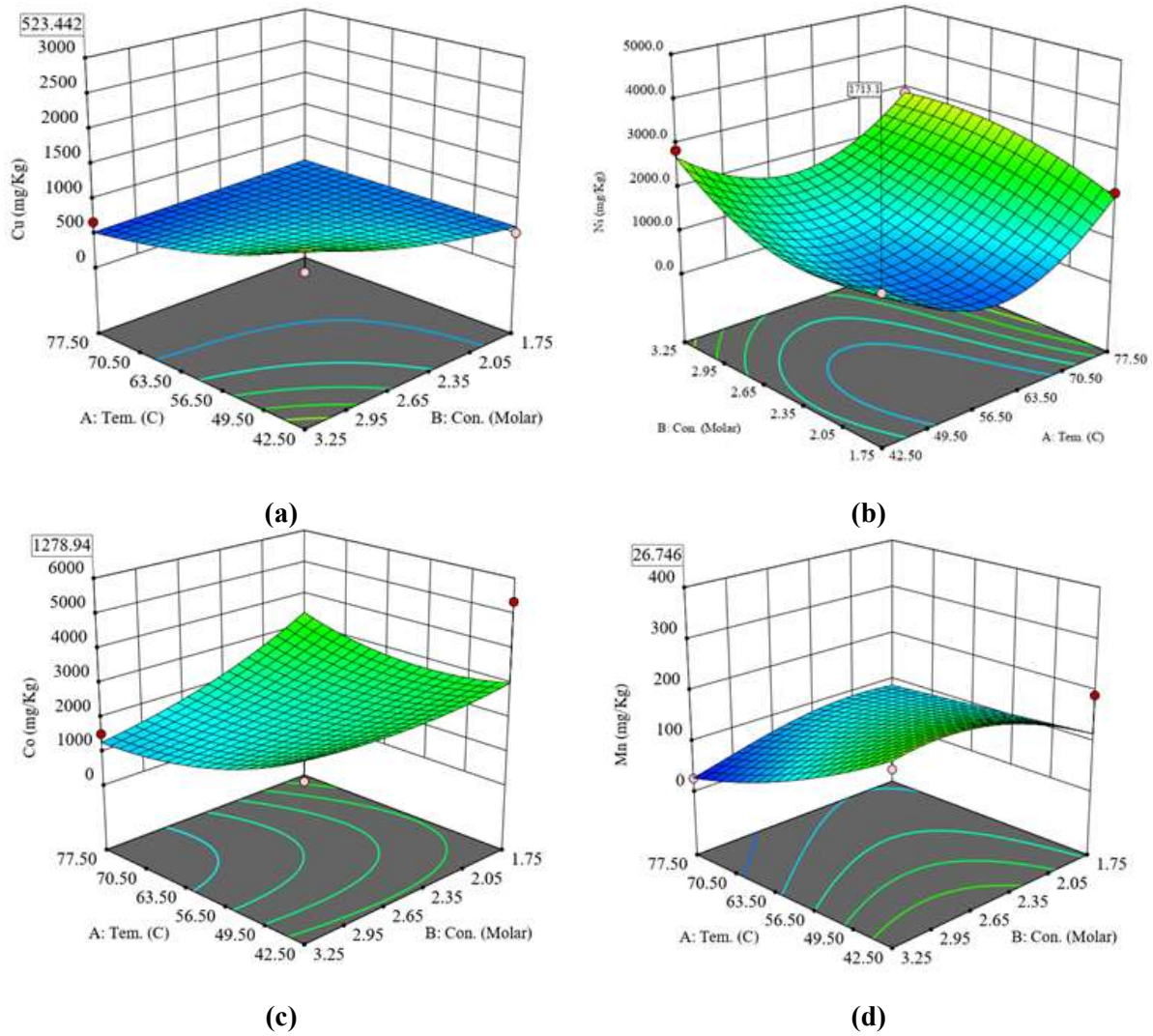


**Figure 5.** Response surface diagrams for a) copper, b) nickel, c) cobalt, d) manganese under optimal conditions.

Based on Figure 5, the optimal conditions for achieving the lowest content of each impurity were obtained and reported in Table 7.

The experiments under the reported optimal conditions were repeated with minimum 3 independent replicates. The results in Table 6 are the mean concentrations of impurities. However, the mean ± standard deviations for the concentration of impurities are given in Table 7.

The response surface diagrams related to the pairwise effects of variables on the percentage of the purity are shown in Figure 6.

**Table 7.**
Minimum impurity content under the optimal conditions.

| Impurity | Impurity concentration (ppm) | L/S | time (hr) | Concentration of sulfuric acid solution (M) | Temperature (ºC) |
|---|---|---|---|---|---|
| Cu | 523±14 | 5 | 4 | 3.25 | 78 |
| Ni | 486±9 | 5 | 4 | 1.9 | 60 |
| Co | 1761±31 | 5 | 4 | 1.75 | 60 |
| Mn | 14.4±0.5 | 7 | 2 | 3.25 | 78 |

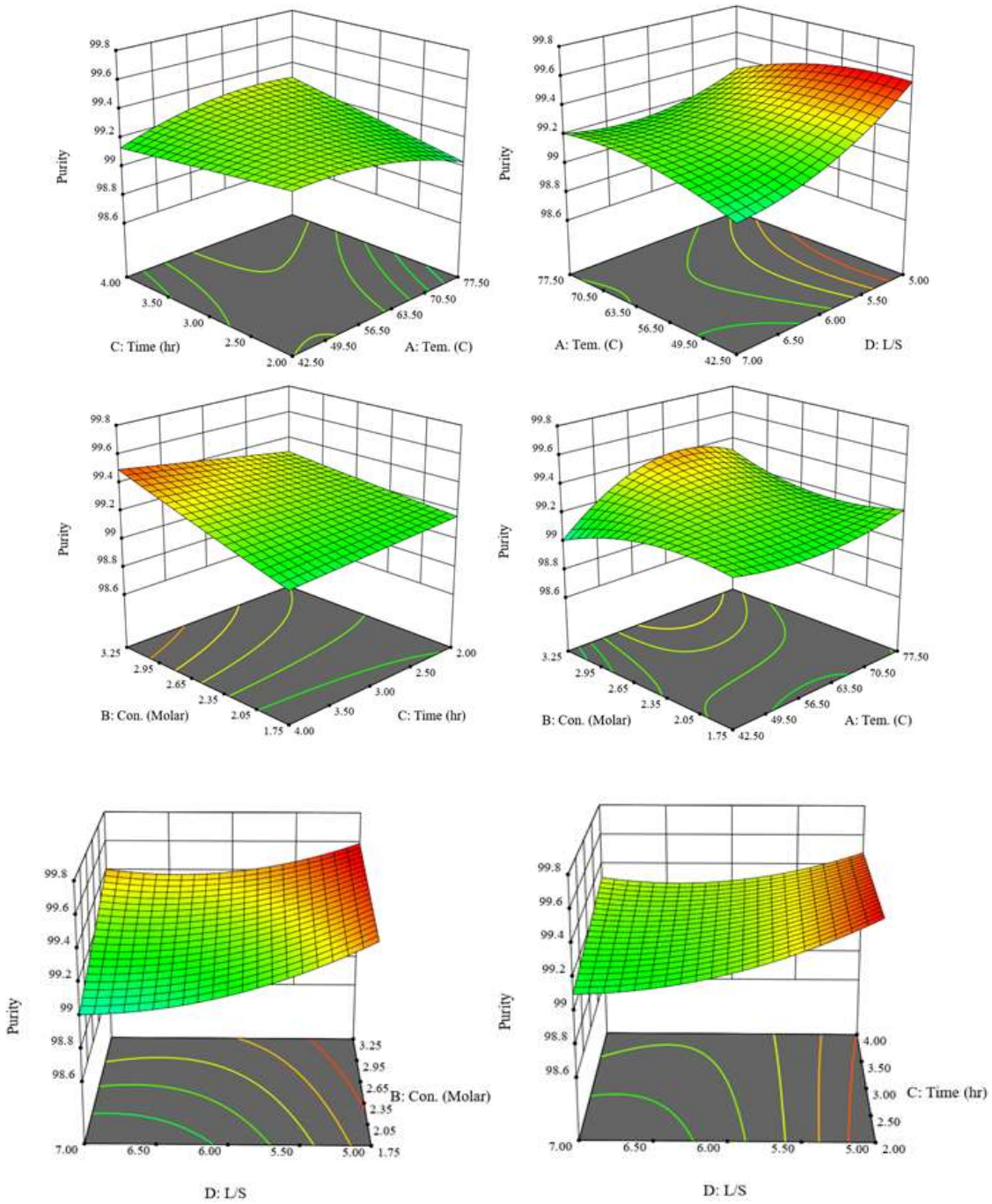


**Figure 6.** Response surface plots for the effects of variables in pairs on the percentage of the purity.

Figure 6 (a) shows the effect of temperature and time on the percentage of the purity. According to this figure, changes in temperature and time do not have much increasing effect on the purity. However, increasing the concentration of the acid at low temperatures has little effect, but at high temperatures, increasing the concentration of the acid leads to an increase in the percentage of the purity. Figure 6(b) shows the effect of temperature and acid-to-powder ratio. According to this figure, temperature changes at high ratios are small, but at low ratios, the effect of temperature is notable. According to Figure 6(c), increasing the concentration over a long period increases the percentage of the purity linearly. Figure 6(d) shows the effect of temperature and concentration on the percentage of the purity. At low concentrations, the temperature increase trend

is parabolic, initially decreasing and then increasing after the central point, but at high concentrations, this trend is reversed, initially increasing and then decreasing, with greater intensity. Figure 6(e) shows the effect of acid-to-powder ratio and the concentration of the acid on the percentage of the purity. According to this figure, at high ratios, by increasing acid concentration, the percentage of the purity increases with a steeper slope compared to the same at low ratios. Finally, Figure 6(f) shows the effect of the acid to powder ratio and time. At high ratios and with time passage, the percentage of the purity increases with a steep slope, but at low ratios, the effect of increasing the time is negligible. Overall, by examining the trend of changes in all factors to increase the percentage of the purity, the optimal point was obtained.

According to the perturbation diagram shown in Figure 7, the percentage of the purity reaches its maximum value of 99.53% at the temperature of 77 °C, concentration of 1.75 M, time of 4 hours, and acid-to-powder ratio of 5.

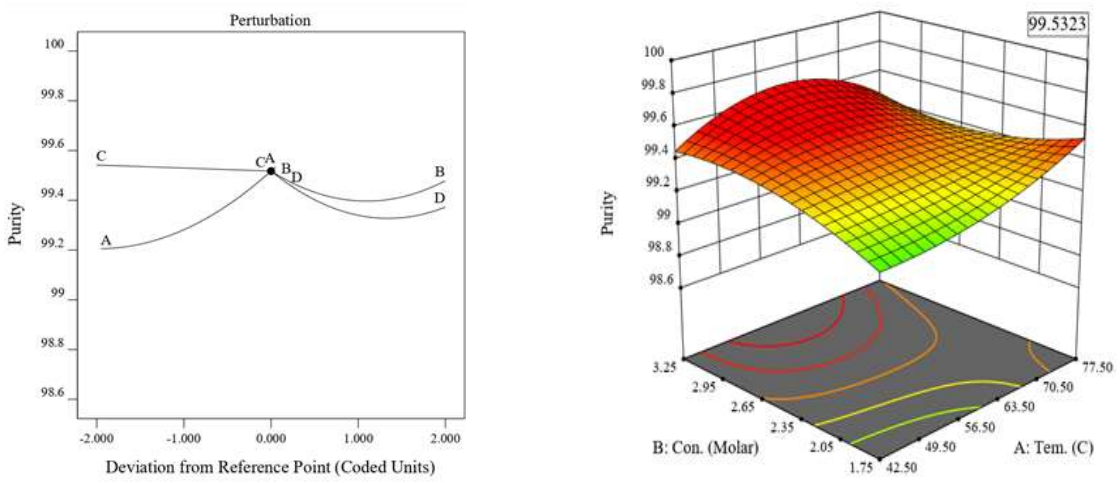


**(a)** **(b)**

**Figure 7.** (a) Perturbation diagram, and (b) Response surface diagram of optimal conditions.

After determining the optimal conditions, a confirmation test was performed. Sampling was performed from the obtained powder, and XRD and ICP tests were conducted, and their results are shown in Figure 8 and Table 8 respectively.

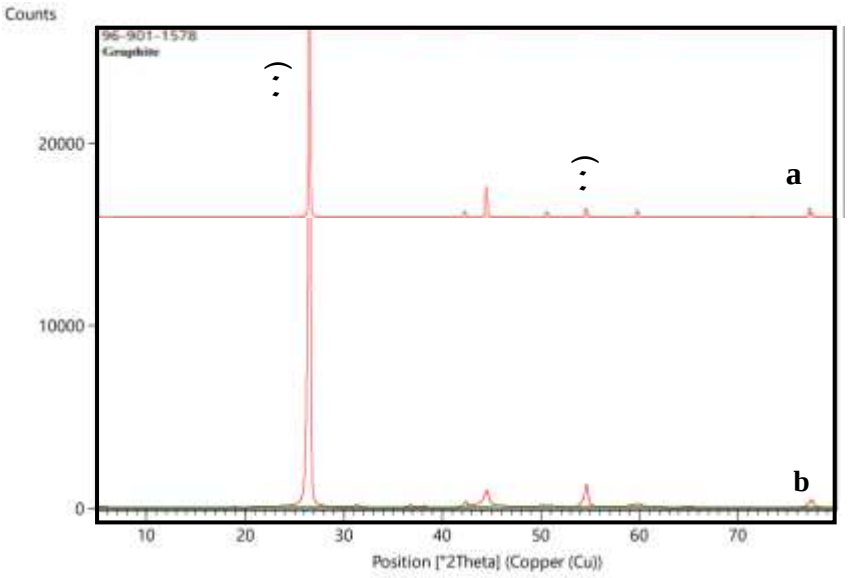


**Figure 8.** X-ray diffraction pattern of a) reference, b) graphite after the first-stage leaching under the optimal conditions.

According to Figure 8, a sharp peak at $2\theta = 26°$ related to the (002) plane and a small peak at $2\theta \approx 53°$ related to the (004) plane of graphite are observed, which relate to the interlayer distance of graphite. The sharpness and intensity of the peak indicate high graphite crystallinity.

**Table 8.**
Graphite impurity values after the first-stage leaching under the optimal conditions.

| Impurity | Composition (wt%) | Concentration (ppm) |
|---|---|---|
| Ni | 0.19±0.04 | 1932.8±35 |
| Co | 0.14±0.02 | 1435.8±25 |
| Cu | 0.05±0.01 | 460.2±12 |
| Mn | 0.02±0.01 | 55.2±2 |
| | 99.61±0.15 | Graphite purity |

According to Table 8, the optimal purity of graphite in the first leaching stage is 99.61%.

### 3.1. Effect of the heat treatment on the purity and structural modification of graphite

The use of heat treatment for regenerating the structure of graphite has been reported in many studies. In most sources, the high-temperature heat treatment using nitrogen and argon atmospheres is used to modify the structure of the spent graphite, increase the XRD peak at 26.5°, and increase initial charge capacity. Using low-temperature sulfation roasting modifies the structure of graphite, reduces remaining impurities in graphite, and also reduces required energy.

As it is seen in Table 8, a significant amount of cobalt, nickel, manganese, and copper still remains in graphite after the leaching operation. To remove these impurities, after filtration, the graphite obtained by leaching with sulfuric acid, without water washing, is mixed with a very small amount of sulfuric acid and then undergoes roasting at 200 °C for 4 hours, with a heating rate of 10 °C/h. In this work, the remaining metals in graphite (nickel, cobalt, manganese, and copper) convert to low-valence sulfates $CoSO_4$, $NiSO_4$, $MnSO_4$, and $CuSO_4$. The obtained metal compounds are easily dissolved in sulfuric acid and lowered in graphite. Consequently, one stage of leaching under initial leaching conditions was considered to remove impurities. Also, after re-leaching with sulfuric acid, the purified graphite is washed with some deionized water to neutralize the acid in

graphite and dissolve impurities, whih are not removed by acid, in water.

Table 9 shows the amount of impurities in graphite after one stage of sulfation roasting and leaching with sulfuric acid. The results showed that metal impurities such as cobalt, nickel, manganese, and copper have significantly decreased. The purity of the recycled graphite is similar to that of the commercial graphite. This result is comparable to the work of Ma et al [17]. This indicates that releaching and heat treatment play an important role in obtaining better results. The advantage of this research is using heat treatment. If the energy cost is significant, the heat treatment is a limitation.

**Table 9.**
ICP analysis results of the spent graphite, graphite after leaching with sulfuric acid, graphite after leaching and heat treatment, and commercial graphite.

| Graphite states | Mn (ppm) | Cu (ppm) | Ni (ppm) | Co (ppm) | C (wt%) |
|---|---|---|---|---|---|
| Spent graphite | 12.582 | 18.048 | 15.341 | 63.171 | 88.51 |
| Graphite after leaching with sulfuric acid | 205 | 509 | 1.784 | 1.529 | 99.61 |
| Graphite after leaching and heat treatment | 18 | 28 | 25 | 28 | 99.97 |
| Commercial graphite | 1.9> | 9.5 | 1.9> | 19 | 99.95 |

Figure 9 shows the XRD results of the spent graphite samples, graphite after leaching and heat treatment, and commercial graphite. As observed, in all three samples, the characteristic peak at $2\theta = 26°$ related to the (002) plane and a small peak at $2\theta \approx 53°$ related to the (004) plane of graphite are seen, which relate to the interlayer distance of graphite. The sharpness and intensity of the peak indicate high crystallinity of graphite. In the SG sample, the peak intensity is very low and differs greatly from the same in the commercial graphite. After performing two stages of leaching and sulfation roasting, the peak intensity at $2\theta = 26.5°$ has increased. Under these conditions, the peak intensity of modified graphite still differs significantly from that of the commercial graphite.

The spent graphite in batteries as electrodes undergo expansion and contraction multiple times due to insertion and extraction of lithium ions and other cations and anions, thus losing the order in raw graphite layers. However, this reduction in crystallinity is due to the separation of graphene layers from each other, which is electrochemically very desirable because, in addition to creating a suitable bed for the insertion of cation and anion, particularly lithium ions, it allows better penetration to the electrolyte and other bulky cations and anions used in the battery, improving battery capacity in addition to its conductivity [15].

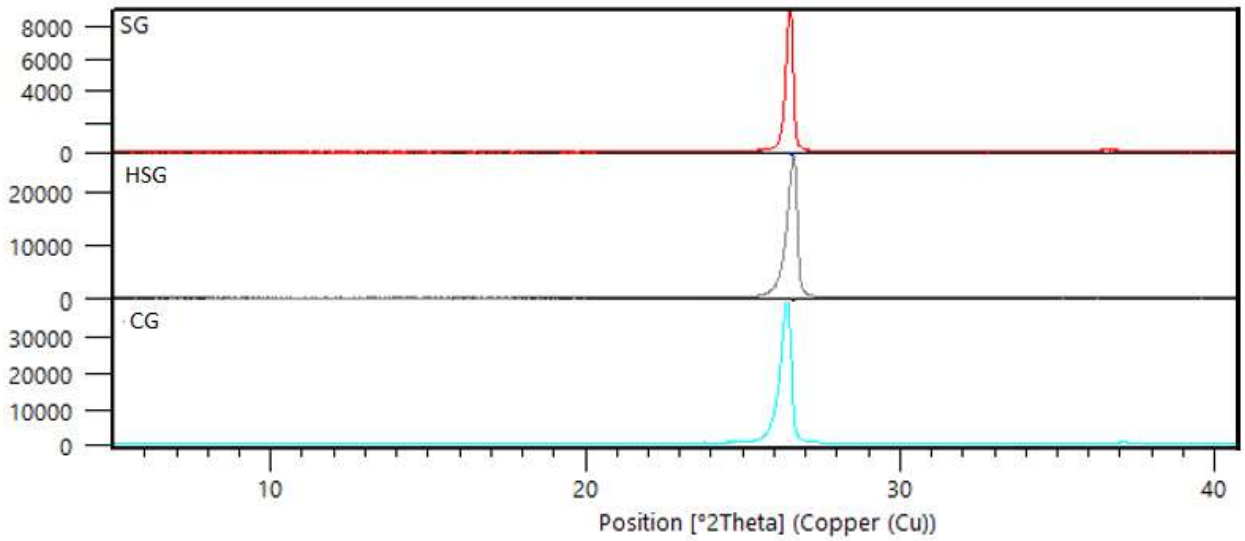


**Figure 9.** XRD results of the spent graphite samples, graphite after leaching and heat treatment, and commercial graphite.

### 3.2. Electrochemical results

In this research, after preparing an electrode, with a slurry containing the sample, and a laboratory cell, including the graphite electrode versus lithium as the reference electrode, were prepared, and a constant current charge-discharge program of 0.2 A was applied to the cell. From the graphite obtained by the sulfuric acid leaching process, sulfation roasting, and re-leaching with sulfuric acid, an electrode was prepared, and charge-discharge and cyclicity tests were performed. Results are shown in Figure 10. According to this figure, an initial capacity of 345±3 mAh/g was obtained at the current of 0.3 mA; however, in subsequent cycles, the capacity instability may be related to the presence of impurities and the unstable structure of graphite. After 5 cycles, it was stabilized at 300±3 mAh/g, and it was predicted that up to the 100th cycle, 89±1% capacity will be retained.

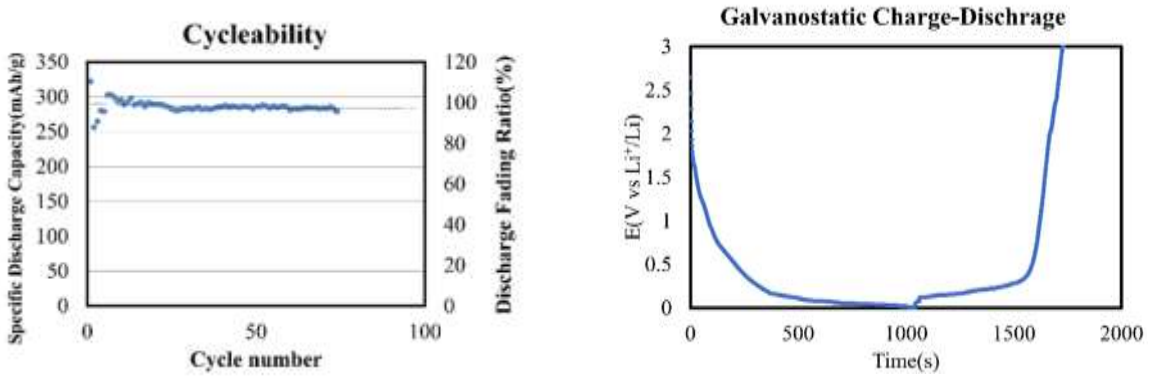


**(a)** **(b)**

**Figure 10.** (a) Cyclicity diagram, and (b) Constant current charge-discharge diagram.

As it can be seen in Figure 10, the graphite obtained from the process has a significant drop in the charge and discharge capacity. Consequently, it does not possess the electrochemical properties required for lithium-ion battery anodes. To improve electrochemical properties, the recovering process was repeated, and the electrochemical

results of the obtained graphite are shown in Figure 11. According to Figure 11(a), the discharge diagram starts decreasing from 3 V because the open circuit potential at near 3 V relates to the potential difference between graphite (positive electrode) and lithium (negative electrode). The discharge current causes the intercalation of lithium-ion into graphite layers, and thus the potential tends to zero. The potential being reduced to 0.35 V relates to the intercalation process of lithium-ion between graphite layers. With further reduction in the potentialvalue, the lithium-carbon compound ($LiC_6$) is formed. Then, the charge current performs the reverse operation with energy expenditure to return the potential difference to 3 V. The battery capacity is calculated from the area under the discharge curve. This electrode showed the 450±3 mAh/g capacity in the first cycle, which dropped slightly in subsequent cycles and stabilized relatively at 350±3 mAh/g. In similar research by Ma et al [17], a 377.3 mAh/g capacity in the first cycle was obtained. They admitted that their purification processes were not very good and could be improved. This was pointed in section 3.1. The data for the commercial graphite in the first cycle is 372±3 mAh/g.

Considering that the commercial graphite also has the capacity of approximately 350±3 mAh/g, it can be stated that the spent graphite that has undergone hundreds of different charge and discharge cycles can be recovered to an acceptable extent through calcination and leaching processes.

Repeating charge and discharge based on the number of cycles creates the cyclicity diagram shown in Figure 11(b). According to the cyclicity diagram, although the capacity has slightly decreased in multiple cycles, increasing reliability, it has a relatively severe initial 20% drop. This phenomenon usually occurs when the structure of graphite is unstable, and after lithium ions intercalate into graphite, the capacity increases greatly, but upon extraction, 20% of them are trapped and no longer usable. This causes capacity reduction in subsequent cycles because the lithium ions are consumed and also part of the structure of graphite becomes inaccessible.

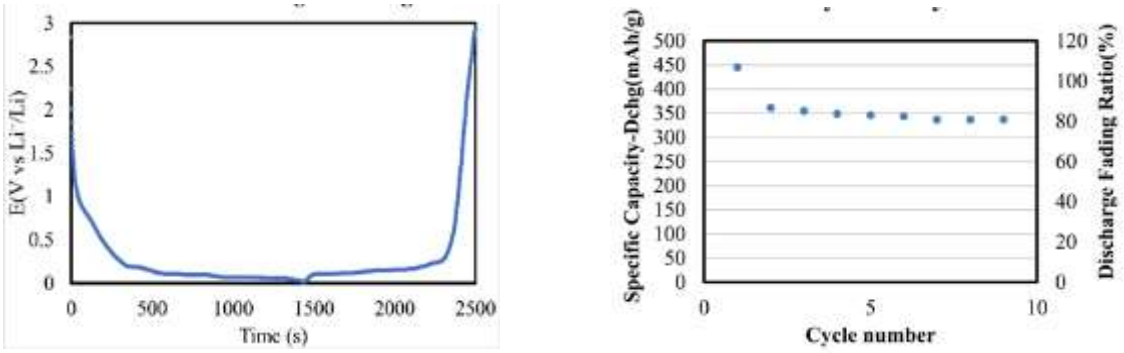


**(a)** **(b)**

**Figure 11.** (a) Constant current charge-discharge diagram, and (b) cyclicity diagram.

## 4. Conclusions

In the operation of recovering graphite from spent batteries (which use processes such as the initial drying of graphite to remove moisture, milling, burning plastics along with graphite in a furnace, leaching with sulfuric acid, washing graphite with sulfuric acid and sulfation roasting, leaching roasted graphite, and finally drying the leached roasted product), the primary and secondary leaching processes are important. Therefore, these two processes were optimized. The optimal conditions in primary leaching consist of the temperature of 77 °C, concentration of 1.75 M

of sulfuric acid, duration of 4 hours, and sulfuric acid to graphite powder ratio of 5. The graphite purity in the primary leaching process is 99.61%.

To remove remaining impurities, the graphite obtained from the first leaching stage is mixed with a very small amount of sulfuric acid and then undergoes roasting at 200 °C, for of 4 hours at a heating rate of 10 °C/h. The remaining elements in graphite (nickel, cobalt, manganese, and copper), under the mentioned roasting conditions, are converted to low-valence sulfates $CoSO_4$, $NiSO_4$, $MnSO_4$, and $CuSO_4$. The obtained metal compounds are easily dissolved in sulfuric acid, reducing the amount of impurities in graphite. The purity of the resulting graphite is 99.97%. To evaluate the electrochemical behavior, galvanostatic charge-discharge tests were performed, and according to the obtained results, a capacity of 350 mAh/g was achieved, which is similar to that of the commercial graphite.

## List of Symbols

| | |
|---|---|
| A | Temperature (°C) |
| B | Acid concentration (M) |
| C | Washing time (hr) |
| D | Ratio of solid graphite to acidic solution (-) |
| S/L | Ratio of solid graphite to acidic solution (-) |

## Author Contributions

The contributions of each individual author are:

**Ramin Badrnezhad:** Conceptualization, investigation, sourcing, supervision, funding acquisition,

**Mohammad Mahdi Bahri:** Conceptualization, presenting methodology, investigation, writing—reviewing and editing, visualization,

**Mobin Gharemanlou:** Conducting formal analysis, investigation, writing—original draft preparation

**Mehrdad Shourehkandi:** Conducting formal analysis

**Shahram Ghanbari:** Conceptualization, presenting methodology, investigation, writing—original draft preparation, writing-reviewing and editing, visualization, supervision, project administration

**Maryam Farid Mohammadi:** software, validation, Conducting formal analysis, investigation, data curation

## Conflict of interest

The authors declare no conflict of interest.

## References

[1] Kazazi M, Karimi S, Ashtari P (2024) Using Tangerine Peel as a Reducing Agent in the Process of Recovering the Cathode Elements from Spent Lithium-Ion Batteries. *Iranian Journal of Chemistry and Chemical Engineering* 43(10):3628–3641. https://doi.org/10.30492/ijcce.2024.2023387.6454

[2] Daraei M, Sadegh Hasani S, Samiei L (2019) Application of Graphene for Clean Energy Production. *Iranian Chemical Engineering Journal* 18(102):50–64. https://doi.org/20.1001.1.17355400.1398.18.102.5.8

[3] Bahri M.M, Ghahremanlou M, Badrnezhad R, Ghanbari S (2023) Effective Parameters on High-Purity Lithium Carbonate Production from Spent Lithium-Ion Batteries. *Iranian Journal of Chemistry and Chemical Engineering* 42(9):2886–2894. https://doi.org/10.30492/ijcce.2023.1973856.5727

[4] Yang Y, Song S, Lei S, Sun W, Hou H, Jiang F, Ji X, Zhao W, Hu Y (2019) A Process for Combination of Recycling Lithium and Regenerating Graphite from Spent Lithium-Ion Battery. *Waste Management* 85:529–537. https://doi.org/10.1016/j.wasman.2019.01.008

[5] Traore N, Kelebek S (2023) Characteristics of Spent Lithium-Ion Batteries and Their Recycling Potential Using Flotation

Separation: A Review. *Mineral Processing and Extractive Metallurgy Review* 44(3):231–259. https://doi.org/10.1080/08827508.2022.2040497

[6] Yi C, Yang Y, Zhang T, Wu X, Sun W, Yi L (2020) A Green and Facile Approach for Regeneration of Graphite from Spent Lithium-Ion Battery. *Journal of Cleaner Production* 277:123585. https://doi.org/10.1016/j.jclepro.2020.123585

[7] Liu J, Shi H, Hu X, Geng Y, Yang L, Shao P, Luo X (2022) Critical Strategies for Recycling Process of Graphite from Spent Lithium-Ion Batteries: A Review. *Science of the Total Environment* 816:151621. https://doi.org/10.1016/j.scitotenv.2021.151621

[8] Cheng Q, Marchetti B, Chen X, Xu S, Zhou X (2022) Separation, Purification, Regeneration and Utilization of Graphite Recovered from Spent Lithium-Ion Batteries: A Review. *Journal of Environmental Chemical Engineering* 10(2):107312. https://doi.org/10.1016/j.jece.2022.107312

[9] Chagnes A, Pospiech B (2013) A Brief Review on Hydrometallurgical Technologies for Recycling Spent Lithium-Ion Batteries. *Journal of Chemical Technology & Biotechnology* 88(7):1191–1199. https://doi.org/10.1002/jctb.4053

[10] Siqi Z, Guangming L, Wenzhi H, Juwen H, Haochen Z (2019) Recovery Methods and Regulation Status of Waste Lithium-Ion Batteries in China: A Mini Review. *Waste Management & Research* 37(11):1142–1152. https://doi.org/10.1177/0734242X19857130

[11] Niu B, Xiao J, Xu Z (2022) Advances and Challenges in Anode Graphite Recycling from Spent Lithium-Ion Batteries. *Journal of Hazardous Materials* 439:129678. https://doi.org/10.1016/j.jhazmat.2022.129678

[12] Yi C, Zhou L, Wu X, Sun W, Yi L, Yang Y (2021) Technology for Recycling and Regenerating Graphite from Spent Lithium-Ion Batteries. *Chinese Journal of Chemical Engineering* 39:37–50. https://doi.org/10.1016/j.cjche.2021.09.014

[13] Guo Y, Li F, Zhu H, Li G, Huang J, He W (2016) Leaching Lithium from the Anode Electrode Materials of Spent Lithium-Ion Batteries by Hydrochloric Acid (HCl). *Waste Management* 51:227–233. https://doi.org/10.1016/j.wasman.2015.11.036

[14] Zhang Z, Zhu X, Hou H, Tang L, Xiao J, Zhong Q (2022) Regeneration and Utilization of Graphite from the Spent Lithium-Ion Batteries by Modified Low-Temperature Sulfuric Acid Roasting. *Waste Management* 150:30–38. https://doi.org/10.1016/j.wasman.2022.06.037

[15] Zhu X, Xiao J, Mao Q, Zhang Z, You Z, Tang L, Zhong Q (2022) A Promising Regeneration of Waste Carbon Residue from Spent Lithium-Ion Batteries via Low-Temperature Fluorination Roasting and Water Leaching. *Chemical Engineering Journal* 430:132703. https://doi.org/10.1016/j.cej.2021.132703

[16] Liu D, Qu X, Zhang B, Zhao J, Xie H, Yin H (2022) Alkaline Roasting Approach to Reclaiming Lithium and Graphite from Spent Lithium-Ion Batteries. *ACS Sustainable Chemistry & Engineering* 8:5739–5747. https://doi.org/10.1021/acssuschemeng.1c07852

[17] Ma X, Chen M, Chen B, Meng Z, Wang Y (2019) High-Performance Graphite Recovered from Spent Lithium-Ion Batteries. *ACS Sustainable Chemistry & Engineering* 7:19732–19738. https://doi.org/10.1021/acssuschemeng.9b05003

[18] Gao Y, Zhang J, Jin H, Liang G, Ma L, Chen Y, Wang C (2022) Regenerating Spent Graphite from Scrapped Lithium-Ion Battery by High-Temperature Treatment. *Carbon* 189:493–502. https://doi.org/10.1016/j.carbon.2021.12.053

[19] Kai Y, Zejun Z, Xin X, Zhongliang T, Ke P, Yanqing L (2019) Graphitic Carbon

Materials Extracted from Spent Carbon Cathode of Aluminum Reduction Cell as Anodes for Lithium-Ion Batteries: Converting the Hazardous Wastes into Value-Added Materials. *Journal of the Taiwan Institute of Chemical Engineers* 104:201–209. https://doi.org/10.1016/j.jtice.2019.09.012

[20] Cao N, Zhang Y, Chen L, Chu W, Huang Y, Jia Y, Wang M (2021) An Innovative Approach to Recover Anode from Spent Lithium-Ion Battery. *Journal of Power Sources* 483:229163. https://doi.org/10.1016/j.jpowsour.2020.229163

[21] Zhang J, Li X, Song D, Miao Y, Song J, Zhang L (2018) Effective Regeneration of Anode Material Recycled from Scrapped Li-Ion Batteries. *Journal of Power Sources* 390:38–44. https://doi.org/10.1016/j.jpowsour.2018.04.039

[22] Yi C, Ge P, Wu X, Sun W, Yang Y (2022) Tailoring Carbon Chains for Repairing Graphite from Spent Lithium-Ion Battery Toward Closed-Circuit Recycling. *Journal of Energy Chemistry* 72:97–107. https://doi.org/10.1016/j.jechem.2022.05.002

[23] He Y, Zhang T, Wang F, Zhang G, Zhang W, Wang J (2017) Recovery of LiCoO2 and Graphite from Spent Lithium-Ion Batteries by Fenton Reagent-Assisted Flotation. *Journal of Cleaner Production* 143:319–325. https://doi.org/10.1016/j.jclepro.2016.12.106

[24] Amer Ali D, Essam Ibrahim M (2024) Optimization Using Central Composite Design for Continuous Absorption of $CO_2$ Gas with Green Sodium Silicate in a Packed Bed Column. *Heliyon* 10(12):e32953. https://doi.org/10.1016/j.heliyon.2024.e32953

[25] Kochar C, Taneja L, Yadav P.K, Tripathy S.S (2024) RSM–CCD Approach for Optimization Study on Effective Remediation of Lead and Cadmium from Water Using Surface-Modified Water Caltrop Peel Biochar. *Biomass Conversion and Biorefinery* 14:17985–18003. https://doi.org/10.1007/s13399-023-04013-2